Available online at www.sciencedirect.com
ScienceDirect
Journal of Photochemistry and Photobiology A: Chemistry 194 (2008) 11–19
Journal of Photochemistry and Photobiology A:Chemistry
www.elsevier.com/locate/jphotochem

Preparation of nanosized TiO_2/ZnO composite catalyst and its photocatalytic activity for degradation of methyl orange

D.L. Liao, C.A. Badour, B.Q. Liao *

Department of Chemical Engineering, Lakehead University, 955 Oliver Road, Thunder Bay, Ont., Canada P7B 5E1

Received 5 April 2007; received in revised form 9 July 2007; accepted 10 July 2007
Available online 17 July 2007

Abstract

The shape and size of TiO_2/ZnO composite nanoparticles can be manipulated by introducing surfactants and different Zn/Ti(OBu)$_4$ molar ratios during the synthesis process. Different sizes of spherical TiO_2/ZnO composite nanoparticles are obtained when sodium dodecyl benzene sulfonate (DBS) and different Zn/Ti(OBu)$_4$ molar ratios are used. Cubic TiO_2/ZnO composite nanoparticles, hexagonal nanorods, and nanobelts are obtained when sodium dodecyl sulfonate (SDS) and different Zn/Ti(OBu)$_4$ molar ratios are used. The XRD study shows that there is no obvious difference in crystal composition of various shapes of TiO_2/ZnO composite nanoparticles. The photocatalytic degradation of methyl orange shows significant variation in rate that decreases in the order: TiO_2/ZnO composites >TiO_2 (with surfactant but no Zn) >TiO_2 (without surfactant and Zn). An optimal Zn/Ti(OBu)$_4$ molar ratio of 0.25:1 is found to achieve the highest photocatalytic activity of TiO_2/ZnO composite nanoparticles.

Keywords: TiO_2/ZnO composite nanoparticles; Shape control; Photocatalytic activity

1. Introduction

TiO_2 nanoparticles have been proved to be an important photocatalyst for degradation of environmental contaminants [1,2]. However, there are still a lot of problems needed to be solved in practical applications of TiO_2 nanoparticles for photocatalysis. For most of the photocatalytic decomposition processes, photonic efficiency is less than 10% [3]. Furthermore, photocatalytic reactions on TiO_2 nanoparticles can usually be induced only by ultraviolet light, which limits the application of TiO_2 as a photocatalyst with visible light. Moreover, the electronic excitation of TiO_2 nanoparticles needs a higher input energy when the particle size decreases because of the quantum size effect [4–6]. Therefore, it is highly desirable to synthesize TiO_2 nanoparticles with a high photocatalytic activity.

One way to improve the photocatalytic activity of TiO_2 nanoparticles is the manipulation of shape, size and surface properties of TiO_2 nanoparticles [7]. Studies have shown that the size and shape of nanoparticles are correlated to the photocatalytic activity of semiconductor nanoparticles [2,3,8–11]. Among the approaches for shape and size manipulation of nanoparticles, one approach is the addition of surfactants, known as "oriented attachment" [5,12], during synthesis [5,12–14].

Another way to enhance the photocatalytic activity is the coating and doping of other materials, including metal ions and semiconductors, onto the surface of TiO_2 nanoparticles [15–17]. The coupling of two semiconductors provides a novel approach to achieve a more efficient charge separation, an increased lifetime of the charge carriers, and an enhanced interfacial charge transfer to adsorbed substrates [18,19]. Recently, studies have shown that the use of TiO_2/WO_3 and TiO_2/MoO_3 composites significantly enhanced the degradation rate of 1,4-dichlorobenzene [20,21]. Other TiO_2 composite nanoparticles, including TiO_2/Fe_2O_3, TiO_2/SiO_2 TiO_2/ZrO_2 [22], TiO_2/In_2O_3 [23], $TiO_2/ZnFe_2O_4$ [24], have also been studied.

The photocatalytic properties of TiO_2/ZnO composite photocatalysts remain largely unexplored although a few studies focused on TiO_2/ZnO composites [25–27]. There is still not much quantitatively known about the regulation of photocatalytic activity of TiO_2 composite nanoparticles. In our previous study, we found that the use of surfactant can manipulate the shape and size of TiO_2 nanoparticles, which leads to an enhanced photocatalytic activity [28]. The ultimate goal of this study is to further improve the photocatalytic activity of TiO_2 nanoparti-

* Corresponding author. Tel.: +1 807 343 8437; fax: +1 807 343 8928.
E-mail address: bliao@lakeheadu.ca (B.Q. Liao).

1010-6030/$ – see front matter © 2007 Elsevier B.V. All rights reserved.
doi:10.1016/j.jphotochem.2007.07.008

cles through a combination of different approaches (composite and surfactant). In this communication, we report the results of photocatalytic activity improvement of TiO_2 nanoparticles through composite with ZnO and surfactant assisted shape and size control.

2. Experiment

TiO_2 and TiO_2/ZnO composite nanoparticles were prepared through the sol–gel method with the introduction of surfactants. Titanium butoxide ($Ti(OC_4H_9)_4$ or $Ti(OBu)_4$, 97%), zinc nitrate hexahydrate ($Zn(NO)_3{\cdot}6H_2O$), ethanol, sodium dodecyl benzene sulfonate (DBS), and sodium dodecyl sulfonate (SDS) were purchased from Sigma–Aldrich Ltd. and used without further purification. Double distilled and deionized water was used throughout this research.

$Ti(OBu)_4$ was dissolved in ethanol with a $Ti(OBu)_4$/ethanol molar ratio of 1:10. The pH of the solution was adjusted to 2.0 with HCl. Surfactant (DBS or SDS) was dissolved in ethanol according to a setting molar ratio and fed into the $Ti(OBu)_4$ solution slowly (0.5 mL/min). In this study, the molar ratio of surfactant to $Ti(OBu)_4$ was fixed at 0.02:1 for SDS and 5:1 for DBS, respectively. These molar ratios were used because of the highest photocatalytic activity was obtained with these molar ratios in our previous study [29]. One mole per liter of $Zn(NO)_3{\cdot}6H_2O$ solution was added into the $Ti(OBu)_4$/surfactant mixture slowly with a setting molar ratio (0.1:1 to 0.5:1) of Zn to $Ti(OBu)_4$. After that, the $Ti(OBu)_4$/surfactant mixture was fed into a mixture of deionized water/ethanol ($Ti(OBu)_4$:water:ethanol molar ratio = 1:4:10, 0.5 mL/min). Hydrolysis reaction and polymerization took place in this mixture and TiO_2 sol was formed. After gelation for 24 h, the gel was dried at 70 °C in an oven until yellow crystal was obtained. After calcined in a muffle furnace at a high temperature (600–800 °C), white TiO_2 nanoparticles were obtained.

The microstructure and morphology of the TiO_2 nanoparticles were observed using a scanning electron microscope (SEM), JEOL5900/OXFORD SEM/EDS. An XRD scan of the nanoparticles was performed using a D/Max III x-ray diffractometer using Cu Kα radiation (Philips). The light reflectance property was studied with a Cary50 UV-VIS-NIR spectrophotometer (Varian Australia PTY Ltd.).

The photocatalytic activity of prepared TiO_2 composite nanoparticles was evaluated in fixed film batch reactors using methyl orange (MO) as a model compound. TiO_2 composite nanoparticles were dispersed in deionized water in a test tube and then treated in an ultrasonic bath (Cole-Parmer Ultrasonic Cleaner, model 08895-16, 100W) for 30 min. Then the suspension was evenly poured onto a 10 cm diameter Petri dish. The dishes were dried in an oven and flushed with deionized water until the pH value of the flushing water became neutral and the weight of the dishes was constant after drying at 105 °C. The loading weight of TiO_2 or TiO_2/ZnO composite nanoparticles in each Petri dish was controlled at 5×10^{-4} g/cm^2. Eighty milliliters of model compound solution was added into the TiO_2 or TiO_2/ZnO composite coated dishes. The solution was mixed by using a magnetic stirrer (1.5 cm in length) at a stirring speed of 60 rpm. The reaction was illuminated by a 6W UV lamp (Blak. Ray UVL 56, wavelength = 365 nm) in a black box. The light intensity was measured by a light intensity meter from Photon Technology International and controlled at 3.0 mW/cm^2 during this study. Solution samples (1 mL/each time) were withdrawn from the fixed film batch reactor for the determination of MO concentration with time and were poured back into the reactor after that. The concentration of MO solution was determined by using a Cary50 UV-VIS-NIR spectrophotometer (Varian Australia PTY Ltd.). The wavelength used for the measurement of MO concentration was 465 nm.

The results of blank experiments under similar conditions but without the addition of catalysts indicated that there was a loss of 1–2% solution volume due to the UV irradiation and reactor open to the air but the loss of substrate was negligible. A comparison of the TiO_2 or TiO_2/ZnO composite catalyst loading weight before and after photocatalytic reaction suggested that 3–5% of fixed TiO_2 or TiO_2/ZnO composite films were sheared out from the Petri dish surface into the solution as suspended particles. For a comparative study of catalytic activity, effect due to this change was not significant.

Photocatalytic reactions on TiO_2 surface can be expressed by the Langmuir–Hinshelwood model [30,31]. The reaction rate after the adsorption equilibrium can be expressed as

$$-\ln\left(\frac{C}{C_0}\right) = Kt \quad (1)$$

where C and C_0 are the reactant concentration at time $t = t$ and $t = 0$, respectively, K and t are the apparent reaction rate constant and time, respectively. A plot of $-\ln(C/C_0)$ versus t will yield a slope of K.

3. Results and discussion

3.1. SEM image analysis

Fig. 1 shows the TiO_2 nanoparticles synthesized from $Ti(OBu)_4$ hydrolysis without using any surfactant and Zn. TiO_2 nanoparticle aggregates with a wide range of size distribution

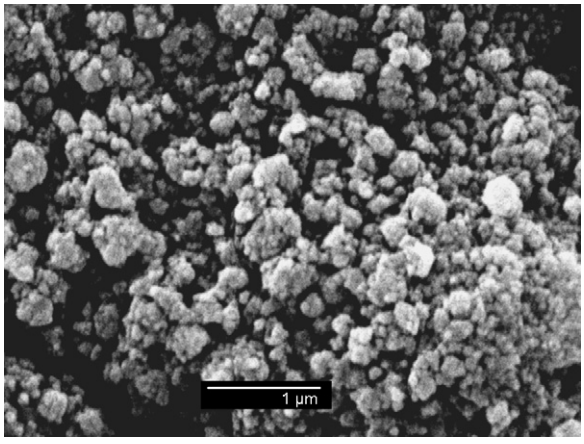

Fig. 1. TiO_2 nanoparticles synthesized from $Ti(OBu)_4$ without using surfactant and Zn addition (bar length = 1 μm).

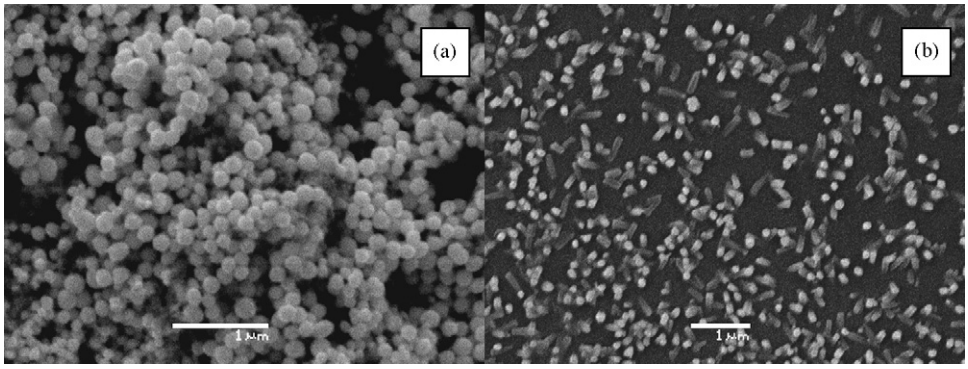

Fig. 2. TiO_2 nanoparticles synthesized from $Ti(OBu)_4$ with the use of surfactants but no Zn addition (bar length = 1 μm). (a) DBS:$Ti(OBu)_4$ = 5:1; (b) SDS:$Ti(OBu)_4$ = 0.02:1.

were formed. The average sizes of TiO_2 nanoparticles ranged from 200 to 300 nm and were irregularly shaped as aggregates. The aggregation could be due to the high viscosity of the sol, which reduced the dispersion of particles.

Effects of DBS and SDS on the shape and size of TiO_2 nanoparticles are shown in Fig. 2. Spherical TiO_2 nanoparticles with a diameter of ∼200 nm were obtained when DBS was used. Well shaped TiO_2 nanorods of ∼100 nm in diameter and ∼500 nm in length were formed when SDS was used. Shape uniformity and size distribution of TiO_2 nanoparticles were improved with the use of surfactants when compared with the nanoparticles in Fig. 1. This could be due to the use of surfactant, which reduced the surface tension of solution and improved the dispersion property of particles.

Fig. 3 shows the TiO_2/ZnO composite nanoparticles shape controlled by DBS at different Zn/$Ti(OBu)_4$ molar ratios. Spherical nanoparticles were formed when DBS was used. Under the SEM, it was observed that size distribution and shape uniformity of TiO_2/ZnO composite nanoparticles were improved with a decrease in the Zn/$Ti(OBu)_4$ molar ratio. The average diameter of the TiO_2/ZnO composite nanoparticles was ∼300 nm. When the Zn/$Ti(OBu)_4$ molar ratios was set at 0.5:1 and 0.25:1, aggregation of the TiO_2/ZnO composite was observed.

Fig. 4 shows the TiO_2/ZnO composite nanoparticles shape controlled by SDS at different Zn/$Ti(OBu)_4$ molar ratios. Cubic nanoparticles at a dimension of 500–1000 nm in length were formed when the Zn/$Ti(OBu)_4$ molar ratio was set at 0.5:1. A shape evolution was observed when the Zn/$Ti(OBu)_4$ molar ratio was increased. Hexagonal nanorods of ∼500 nm in diameter and ∼1500 nm in length were formed when the Zn/$Ti(OBu)_4$ molar ratios was set at 0.25:1. When the Zn/$Ti(OBu)_4$ molar ratio was further decreased to 0.17:1 and 0.1:1, TiO_2/ZnO com-

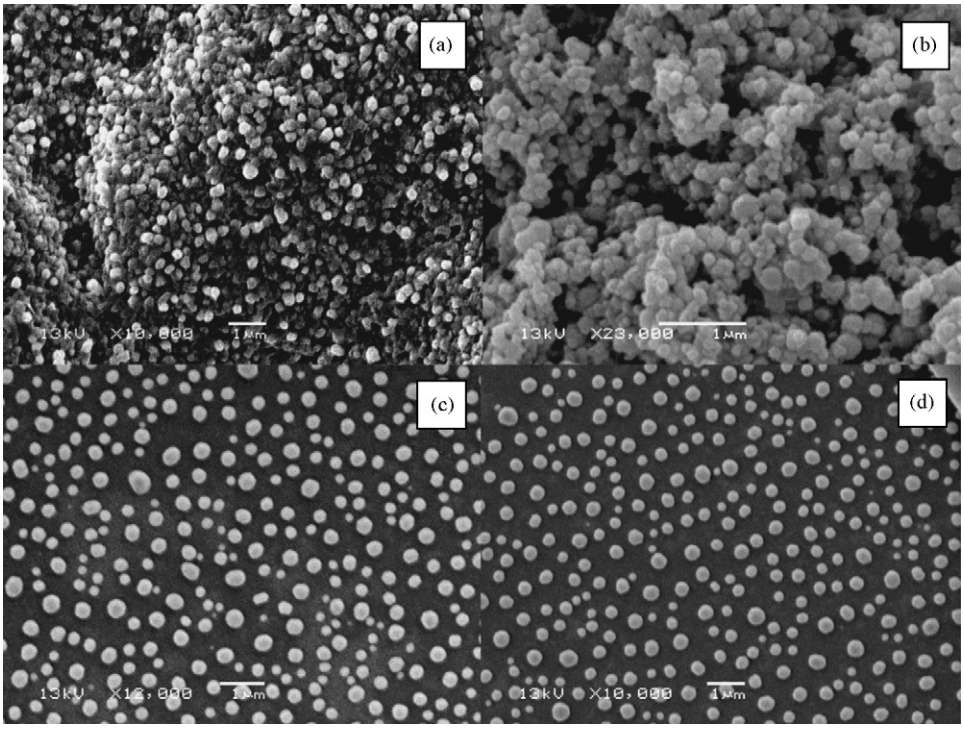

Fig. 3. ZnO/TiO_2 composite nanoparticles synthesized with DBS and a decrease in the Zn/$Ti(OBu)_4$ molar ratio (bar length = 1 μm; calcined at 600 °C, DBS:$Ti(OBu)_4$ = 5:1): (a) 0.5:1; (b) 0.25:1; (c) 0.17:1; (d) 0.1:1.

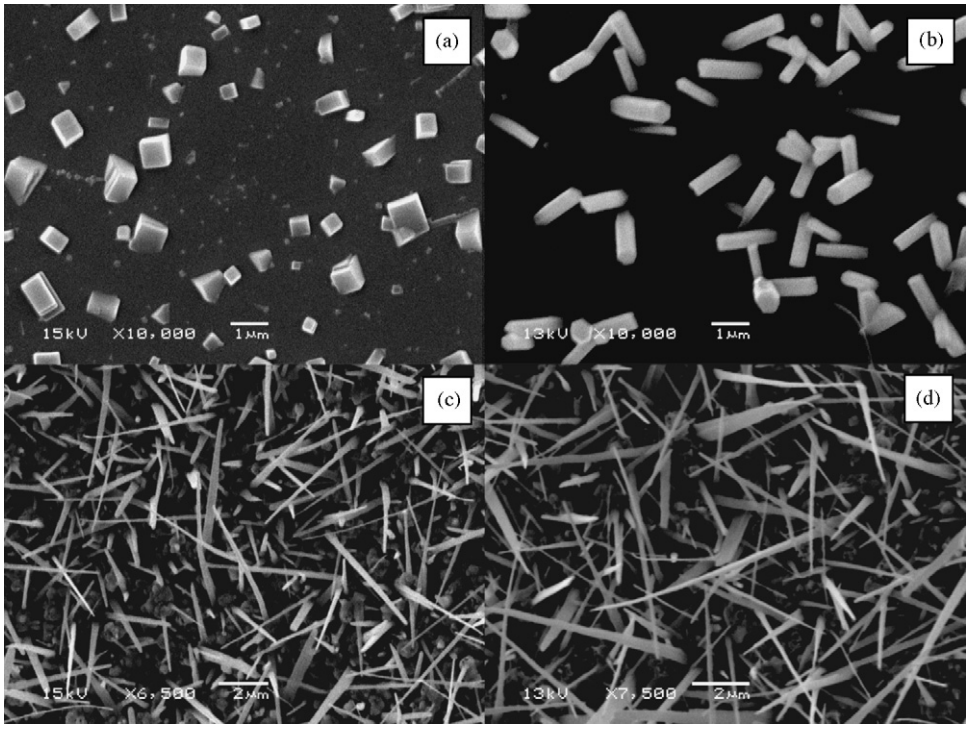

Fig. 4. ZnO/TiO_2 composite nanoparticles synthesized with SDS and a decrease in the Zn/$Ti(OBu)_4$ molar ratio (bar length = 1 μm in (a) and (b) and 2 μm in (c) and (d); calcined at 700 °C, SDS:$Ti(OBu)_4$ = 0.02:1): (a) 0.5:1; (b) 0.25:1; (c) 0.17:1; (d) 0.1:1.

posite nanobelts were formed as shown in Fig. 4(c) and (d). The nanobelts were ~500 nm in width, ~50 nm in thickness and ~8 μm in length.

The hypothesized mechanism of the growth of TiO_2 nanorods and spherical nanoparticles under the action of surfactants is based on the "oriented attachment" and anisotropic and isotropic growth mechanisms [4,32].

The formation and growth of TiO_2 nanoparticles can be described as a two-step process: formation of hydrolysis produces $Ti(OH)_x(OR)_{4-x}$ (monomer structure) and then the polycondensation reactions lead to the formation of a Ti–O–Ti network. Studies have shown that in the absence of surfactant or other additives, titanium alkoxides vigorously react with water at low temperatures [33,34]: amorphous TiO_2 precipitation can be formed. With the presence of surfactants, the surfactant molecules typically comprise a compact Ti–O–Ti network of hexa-coordinated Ti atoms. The Ti nanocrystals are surrounded by carboxylate ligands, which have the propensity to bridge Ti centers. The contact of precursor monomers with water can be hindered when surrounded by surfactants [35] and thus the growth of cross-linking of Ti–O–Ti bonds occurs directionally.

In the presence of surfactants, the limited exposure of –OR groups of titanium alkoxide results in the directional growth of TiO_2 nanoparticles. Nanorods were formed with a high precursor monomer concentration because there was not enough surfactant molecule to block the contact of –OR groups with water in all directions [4]. On the other hand, if some of the conditions favouring directional growth of TiO_2 nanoparticles are retarded, the nanoparticle is nearly spherical or cubic. Through the shape control of the TiO_2 nanoparticles, the chemical and

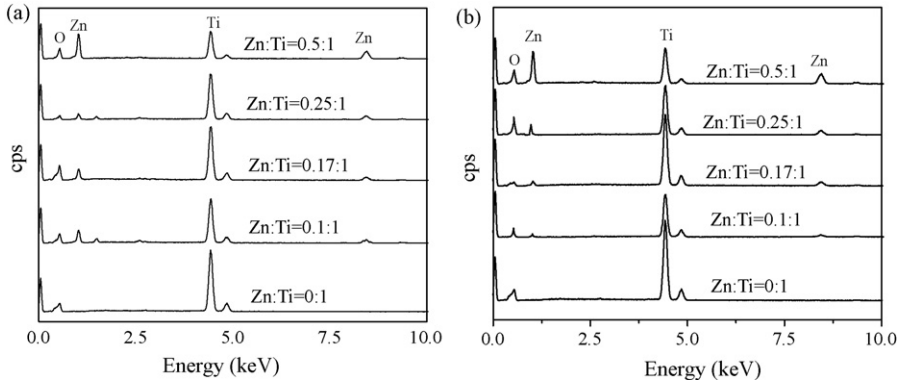

Fig. 5. Energy dispersive X-ray analysis of nanoparticles synthesized with surfactants and Zn addition: (a) nanoparticles synthesized with DBS; (b) nanoparticles synthesized with SDS.

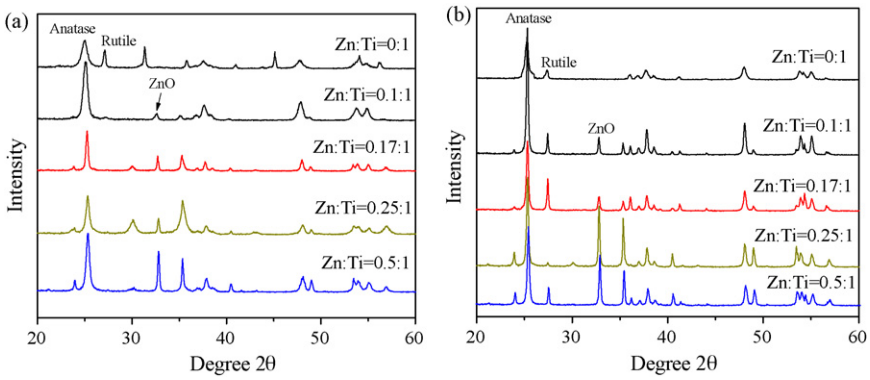

Fig. 6. X-ray diffraction patterns of the nanoparticles synthesized with different Zn/Ti(OBu)$_4$ molar ratios: (a) nanoparticles synthesized with DBS (calcined at 600 °C); (b) nanoparticles synthesized with SDS (calcined at 700 °C).

physical properties can be manipulated. Furthermore, the photocatalytic activity can be regulated.

The potential impact of Zn/Ti(OBu)$_4$ molar ratio on the shape and size is still unknown. On the one hand, similar spherical shape of TiO_2/ZnO composite was obtained at different Zn/Ti(OBu)$_4$ molar ratios, when DBS was used. On the other hand, an evolution in the shape and size of TiO_2/ZnO composite was observed from cubic nanoparticles, nanorods to nanobelts at different Zn/Ti(OBu)$_4$ molar ratios, when SDS was used. It might be caused by a combined effect of both the surfactant and the Zn/Ti(OBu)$_4$ molar ratio and further studies are needed.

3.2. Energy dispersive spectrum (EDS) analysis

Fig. 5 shows the energy dispersion spectra of TiO_2/ZnO composite nanoparticles at different Zn/Ti(OBu)$_4$ molar ratios. The nanoparticles were mainly composed of Ti and O elements. Zn was also observed in the nanoparticles. This suggests that Zn was incorporated into the TiO_2 nanoparticles to form composite. However, the strength of the signal of Zn element was decreased with a decrease in the Zn/Ti(OBu)$_4$ molar ratio. This might not be surprised, as the content of Zn in the TiO_2/ZnO composite could increase with an increase in the Zn/Ti(OBu)$_4$ molar ratio.

3.3. X-ray diffraction characterization

The X-ray diffraction patterns of the TiO_2/ZnO composite nanoparticles at different Zn/Ti(OBu)$_4$ molar ratios were shown in Fig. 6. Although the rutile peak is not obvious due to a compressed scale in some XRD curves in Fig. 6, a small rutile peak does exist in these samples. The calculated anatase percentages of these samples at different Zn/Ti(OBu)$_4$ molar ratios are shown in Table 1. The patterns show that all the nanoparticles consist of anatase as the primary phase. The percentage of rutile component decreased with an increase in the Zn/Ti(OBu)$_4$ molar ratio. The pronounced anatase TiO_2 characteristic diffraction peaks $2\theta = 25.25°$ (1 0 1) and 48.0° (2 0 0) were found in the patterns [2]. The XRD patterns indicate that nanoparticles synthesized without Zn are good crystallinity with the lowest anatase/rutile ratio. ZnO was found in nanoparticles synthesized at different Zn/Ti(OBu)$_4$ molar ratios under the identical conditions. The diffraction intensity of ZnO, as shown in Fig. 6, increased with an increase in the Zn/Ti(OBu)$_4$ molar ratio. This could be due to the improved crystallinity and/or increased concentration of ZnO. There was a small percentage (about 10%) of rutile TiO_2 found in nanoparticles synthesized with a Zn/Ti(OBu)$_4$ molar ratio of 0.25:1 in Fig. 6(a) and (b). It has been reported that the anatase phase has more open structure than the rutile phase, a pure anatase phase is considered to achieve larger surface area, which is necessary to obtain a higher photocatalytic activity [18].

With current knowledge, there is no in-depth explanation on the difference in the percentage of anatase at different surfactant types and concentrations. However, during the formation of TiO_2 nanoparticles, surfactant molecules were attached on the crystal facets of TiO_2 in the sol. The attachment of surfactants changed the surface energy of the TiO_2 crystals. The difference in surface energy of TiO_2 crystal facets affected the anatase formation.

3.4. UV–vis light reflectance analysis

The UV–vis light reflectance spectra of the TiO_2/ZnO composites synthesized at different Zn/Ti(OBu)$_4$ molar ratios are shown in Fig. 7. An obvious red shift of UV–vis reflectance spectra of TiO_2/ZnO composite nanoparticles was observed (spectra 1–4) when compared with the spectrum of neat anatase TiO_2 nanoparticles obtained with the addition of surfactant but no Zn (spectrum 5) and the nanoparticles obtained without the addition of surfactants and Zn (spectrum 6). The results are consistent with the findings of Ohshima et al. [27]. It has been reported that both the band-gap energy of ZnO and that of TiO_2 were of 3.2 eV [36] and the wavelength of the absorption edge of

Table 1
The percentage of anatase component in the TiO_2/ZnO composite at different Zn/Ti(OBu)$_4$ molar ratios

	Anatase (%)				
	0:1[a]	0.1:1[a]	0.17:1[a]	0.25:1[a]	0.5:1[a]
Surfactant					
DBS	55.32	84.90	88.53	90.43	92.81
SDS	80.51	83.43	87.91	89.52	90.27

[a] Zn/Ti.

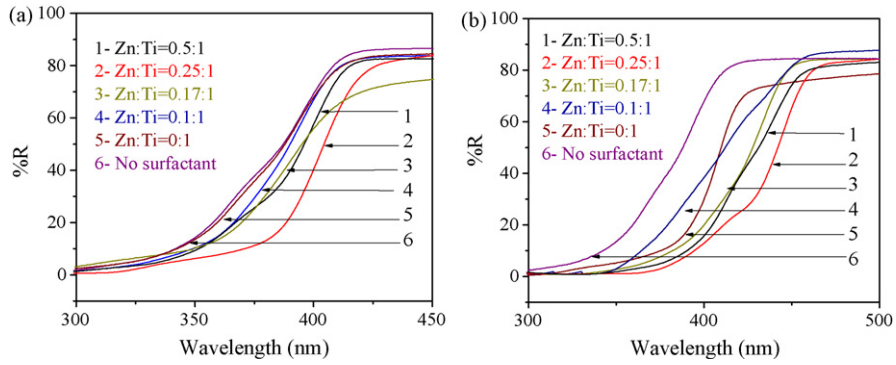

Fig. 7. UV–vis reflectance spectra of the nanoparticles synthesized with different Zn/Ti(OBu)$_4$ molar ratio: (a) nanoparticles synthesized with DBS; (b) nanoparticles synthesized with SDS.

ZnO and TiO_2 was 391 and 365 nm, respectively [19]. Therefore, the red shift of TiO_2/ZnO composite nanoparticles could be attributed to the contribution of each of the oxide component ZnO and TiO_2, according to the XRD results, as shown in Fig. 6. In addition, the red shift might also be due to the change in the crystal phase composition of TiO_2 nanoparticles. Anatase and rutile TiO_2 contained different energy band gaps which lead to different excitation energy for the nanoparticles. It is interesting to note that the difference in the UV–vis spectra between TiO_2 grown with DBS and that without is small, while the spectra are very different when SDS is used. This might be related to the differences in morphology and size of the particles. A similar morphology and size (200–300 nm) of TiO_2 nanoparticles obtained with and without DBS might lead to a similar absorption. While the nanorods of TiO_2 obtained with SDS have a higher surface-to-volume ratio than that of spheres and this could lead to an increased surface area. Nanoparticles, with their increased surface area, provide surface states within the band gap to effectively reduce the band gap [37].

When the DBS was used, TiO_2/ZnO composite nanoparticles strongly absorbed UV light within a wavelength below 380 nm, while the neat anatase TiO_2 nanoparticles absorbed most of the UV light with a lower wavelength (<350 nm). This suggests that the TiO_2/ZnO composite nanoparticles have a lower band gap than the neat anatase TiO_2 nanoparticles. The lower band gap has a positive effect on the photocatalytic activity because

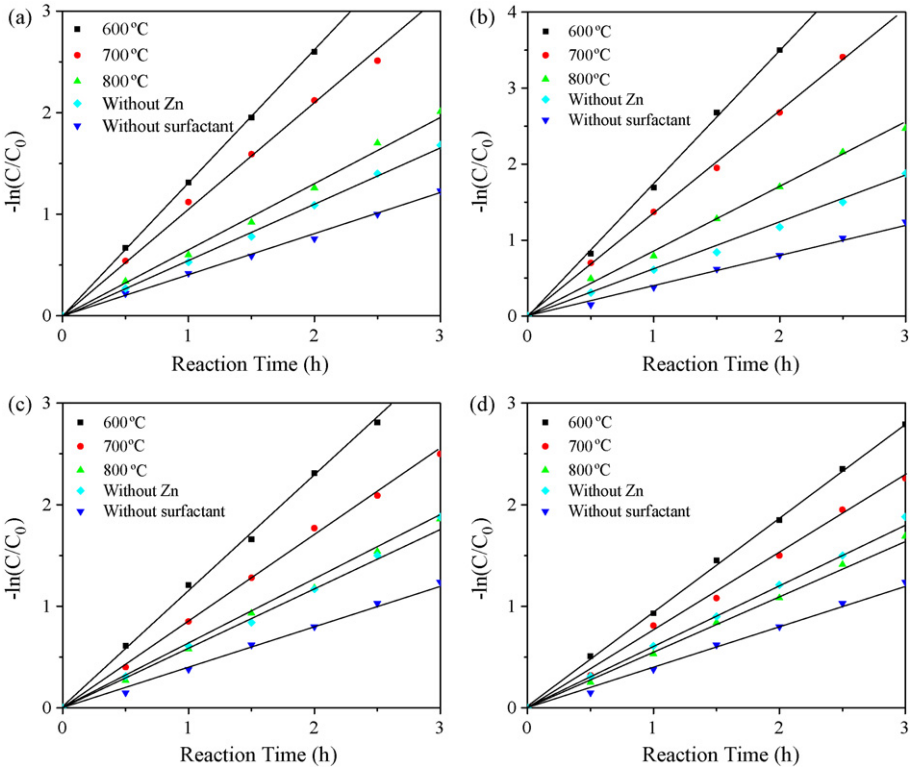

Fig. 8. Relationship between $-\ln(C/C_0)$ and reaction time of MO photocatalytic decomposition with the nanoparticles synthesized with DBS [initial MO concentration 5000 μg/L; calcination temperature: 600 °C for nanoparticles samples without Zn but with surfactant or without surfactant and Zn]. (a) Zn:Ti(OBu)$_4$ = 0.5:1; (b) Zn:Ti(OBu)$_4$ = 0.25:1; (c) Zn:Ti(OBu)$_4$ = 0.17:1; (d) Zn:Ti(OBu)$_4$ = 0.1:1.

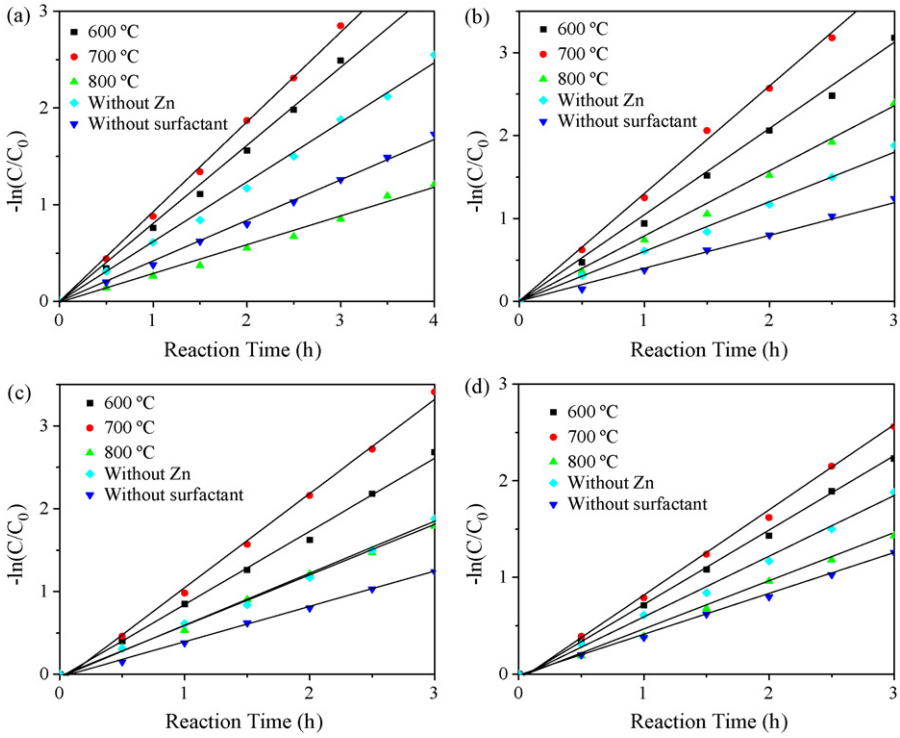

Fig. 9. Relationship between $-\ln(C/C_0)$ and reaction time of MO photocatalytic decomposition with the nanoparticles synthesized with SDS [initial MO concentration 5000 μg/L; calcination temperature: 700 °C for nanoparticle samples without Zn but with surfactant or without surfactant and Zn]. (a) $Zn:Ti(OBu)_4 = 0.5:1$; (b) $Zn:Ti(OBu)_4 = 0.25:1$; (c) $Zn:Ti(OBu)_4 = 0.17:1$; (d) $Zn:Ti(OBu)_4 = 0.1:1$.

lower source energy is needed to arouse a photocatalytic reaction. In the cases of SDS, the TiO_2/ZnO composite nanoparticles (spectra 1–4 in Fig. 7(b)) strongly absorbed the light within a wavelength below 400 nm, which is higher than the ZnO/TiO_2 composite nanoparticles synthesized with DBS (spectra 1–4 in Fig. 7(a)). In both surfactants, the TiO_2/ZnO composite nanoparticles synthesized at a $Zn/Ti(OBu)_4$ molar ratio of 0.25:1 have the largest "red shift" when compared with the neat anatase TiO_2 nanoparticles.

3.5. Photocatalytic activity

Photocatalytic decomposition of methyl orange (MO) was used to evaluate the photocatalytic activities of the synthesized TiO_2/ZnO composite nanoparticles because MO solution is stable under UV illumination (without the use of TiO_2 catalyst) [19]. It is well accepted that the photocatalytic decomposition of organic pollutants accords with a pseudo first-order kinetic [30,31]. The relationships between $-\ln(C/C_0)$ and reaction time are shown in Figs. 8 and 9. The apparent reaction rate constants (K) of MO decomposition using different photocatalysts are summarized in Table 2.

As shown in Table 2, TiO_2/ZnO composite nanoparticles had a higher photocatalytic activity, which was represented by a larger value of K, than the nanoparticles obtained without the addition of Zn. When compared to TiO_2 nanoparticles synthesized without the use of surfactants, the shape-controlled TiO_2 nanoparticles with the use of surfactants showed a higher photocatalytic activity. Among the nanoparticles calcined at different temperatures, the nanoparticles calcined at 600 and 700 °C showed the higher photocatalytic activities under different $Zn/Ti(OBu)_4$ molar ratios for nanoparticles grown with DBS and SDS, respectively. In both cases of using DBS and SDS, the nanoparticles synthesized at a $Zn/Ti(OBu)_4$ molar ratio of 0.25:1 showed the highest photocatalytic activity. The photocatalytic activity results suggest that the shape controlling process

Table 2
Apparent reaction rate constant (K, h^{-1}) of MO photocatalytic decomposition on different nanoparticles

Zn/Ti ratio	DBS:Ti = 5:1			SDS:Ti = 0.02:1		
	600 °C	700 °C	800 °C	600 °C	700 °C	800 °C
Zn:Ti = 0.5:1	1.27	0.87	0.61	0.89	1.03	0.31
Zn:Ti = 0.25:1	1.81	1.40	0.85	1.05	1.25	0.85
Zn:Ti = 0.17:1	1.09	0.84	0.60	0.92	1.14	0.61
Zn:Ti = 0.1:1	0.95	0.76	0.58	0.77	0.88	0.50
Zn:Ti = 0:1	0.57	0.53	0.43	0.59	0.63	0.47
Without surfactant Zn:Ti = 0:1	0.42	0.44	0.40	0.42	0.44	0.40

with surfactant can improve the photocatalytic activity of TiO_2 nanoparticles. Photocatalytic activity of the shape-controlled TiO_2 nanoparticles can be further improved with the composite of ZnO.

The results of improved photocatalytic activity of TiO_2 nanoparticles through composite with ZnO are consistent with the findings of Yang et al. [25], Serpone et al. [38], and Sukharev and Kershaw [39]. The higher photocatalytic activity of TiO_2/ZnO composite nanoparticles is related to the role of ZnO on the surface of TiO_2 nanoparticles [38,39]. The fact can be related to the vectorial transfer of electrons and holes, which takes place in coupled semiconductors possessing different redox energy levels for their corresponding conduction and valence bands [39]. In the TiO_2/ZnO composite, the electron transfer occurs from the conduction of band of light-activated ZnO to the conduction of band of light-activated TiO_2 and, conversely, hole transfer can take place from the valence band of TiO_2 to the valance band of ZnO [38,39]. This efficient charge separation increases the lifetime of the charge carriers and enhances the efficiency of the interfacial charge transfer to adsorbed substrates [39].

The TiO_2/ZnO composite nanoparticles synthesized at a $Zn/Ti(OBu)_4$ molar ratio of 0.25:1 showed the highest photocatalytic activity because these nanoparticles showed the biggest red shift in the UV–vis light reflectance, as shown in Fig. 7(a) and (b), which means these composite nanoparticles have the lowest band gap energy. A previous study showed that an extension of the wavelength range of light absorption increased the photocatalytic activity of TiO_2 nanoparticles [13]. When the $Zn/Ti(OBu)_4$ molar ratio was low (0.17:1 and 0.1:1), the effect of photogenerated electron trapped by ZnO was not obvious because of the insufficiency of ZnO. The photocatalytic activity was thus not the highest. When the $Zn/Ti(OBu)_4$ molar ratio was high (0.5:1), some TiO_2 active sites would be surrounded by ZnO which hinders the contact between TiO_2 and oxygen containing species, which decreased the photocatalytic activity. Thus, an optimal TiO_2/ZnO composition existed for the highest photocatalytic activity.

On the one hand, from Table 2, it is noted that the photocatalytic activity of TiO_2 nanoparticles obtained with SDS but no Zn (Zn:Ti = 0:1) is generally higher than that with DBS but no Zn at different temperatures. This could be attributed to the difference in morphology of TiO_2 nanoparticles. Nanorods from SDS (Fig. 2) have a higher surface-to-volume ratio than nanospheres from DBS with a similar dimension. This would guarantee a higher density of active sites available for surface reactions as well as a higher interfacial charge carrier transfer rate [4].

The effect of temperature (600–800 °C) on the photocatalytic activity is different for TiO_2 nanoparticles obtained with DBS, SDS or without surfactant. From Table 2, it is noted that the photocatalytic activity of TiO_2 nanoparticles obtained with DBS and Zn decreased with an increase in calcination temperature; a maximum photocatalytic activity of TiO_2 nanoparticles obtained with SDS and Zn was observed at 700 °C; and the change in photocatalytic activity is small in terms of calcination temperature for TiO_2 nanoparticles obtained without surfactant and Zn. This could be related to the calcination temperature range tested. In general, there is an optimal calcination temperature for a higher photocatalytic activity, and the optimal calcination temperature changes with respect to the preparation conditions of nanoparticles [40,41]. The small change in the rate of photocatalytic degradation of TiO_2 nanoparticles obtained without the use of surfactant and Zn is within the margin of experimental error (4–10%).

4. Conclusions

Different shapes of TiO_2/ZnO composite nanoparticles, including spherical and cubic nanoparticles, hexagonal nanorods, and nanobelts with different sizes, were prepared by adjusting the $Zn/Ti(OBu)_4$ molar ratio and the introduction of surfactants. SEM images show that the shape and size of the nanoparticles depend not only on the type of surfactant used but also on the $Zn/Ti(OBu)_4$ molar ratio. XRD patterns indicated that there is no obvious difference in crystal structure among different shapes of TiO_2/ZnO composite nanoparticles. Photocatalytic decomposition of MO shows that the TiO_2/ZnO composite nanoparticles have a higher photocatalytic activity than the neat TiO_2 nanoparticles and shape-controlled nanoparticles with surfactants but no Zn. An optimal $Zn/Ti(OBu)_4$ molar ratio of 0.25:1 was found to achieve a higher photocatalytic activity of TiO_2/ZnO composite nanoparticles.

Acknowledgements

This study was supported by the Natural Sciences and Engineering Research Council of Canada (NSERC). The authors wish to thank Dr. G.S. Wu, Department of Chemistry, and Mr. Al Mackenzie, Instrument Laboratory, both at Lakehead University for helps in this study.

References

[1] N.M. Dimitrijevic, Z.V. Saponjic, B.M. Rabatic, T. Rajh, J. Am. Chem. Soc. 127 (2005) 1344–1345.
[2] B.M. Rabatic, N.M. Dimitrijevic, R.E. Cook, Adv. Mater. 18 (2006) 1033–1037.
[3] Z.V. Saponjic, N.M. Dimitrijevic, D.M. Tiede, A.J. Goshe, Adv. Mater. 17 (2005) 965–971.
[4] P.D. Cozzoli, A. Kornowski, H. Weller, J. Am. Chem. Soc. 125 (2003) 14539–14548.
[5] Y. Jun, Y. Jung, J. Cheon, J. Am. Chem. Soc. 124 (2002) 615–619.
[6] A. Peng, X.G. Peng, J. Am. Chem. Soc. 123 (2001) 183–184.
[7] X. Peng, L. Manna, W. Yang, A.P. Alivisatos, Nature 404 (2000) 59–62.
[8] L.A. Gugliotti, D.L. Feldheim, B.E. Eaton, J. Am. Chem. Soc. 127 (2005) 17814–17818.
[9] D. Chatterjee, S. Dasgupta, J. Photochem. Photobiol. C: Photochem. Rev. 6 (2005) 186–205.
[10] N.J. Peill, M.R. Hoffmann, Environ. Sci. Technol. 30 (1996) 2806–2812.
[11] J. Joo, S.G. Kwon, T.K. Yu, J. Phys. Chem. B 109 (2005) 15297–15302.
[12] R.L. Penn, J.F. Banfield, J. Am. Mineral 83 (1998) 1077–1082.
[13] M.P. Pileni, Nat. Mater. 2 (2003) 145–150.
[14] A. Mills, N. Elliot, I.P. Parkin, J. Photochem. Photobiol. A: Chem. 151 (2002) 171–179.
[15] H.M. Yates, M.G. Nolan, D.W. Sheel, M.E. Pemble, J. Photochem. Photobiol. A: Chem. 179 (2006) 213–223.
[16] Y. Bessekhouad, D. Robert, J.-V. Weber, N. Chaoui, J. Photochem. Photobiol. A: Chem. 167 (2004) 49–57.

[17] A. Erkan, U. Bakir, G. Karakas, J. Photochem. Photobiol. A: Chem. 184 (2006) 313–321.
[18] O. Carp, C.L. Huisman, A. Reller, Prog. Solid State Chem. 32 (2004) 33–177.
[19] C. Wang, J. Zhao, X. Wang, Appl. Catal. B: Environ. 39 (2000) 269–279.
[20] L.Y. Shi, C.Z. Li, H.C. Gu, D.Y. Fang, Mater. Chem. Phys. 62 (2000) 62–67.
[21] T. Ohno, F. Tanigawa, S. Izumi, M. Matsumura, J. Photochem. Photobiol. A: Chem. 118 (1998) 41–44.
[22] A.A. Ismail, Appl. Catal. B: Environ. 58 (2005) 115–121.
[23] S.K. Ponyak, D.T. Talapin, A.I. Kulak, J. Phys. Chem. B 105 (2001) 4816–4822.
[24] S. Srinivasan, J. Wade, E.K. Stefanakos, J. Nanomater. 2006 (2006) 1–4 (Article ID 45712).
[25] S.G. Yang, X. Quan, X.Y. Li, Y.Z. Liu, S. Chen, G.H. Chen, Phys. Chem. Chem. Phys. 6 (2004) 659–664.
[26] K.H. Yoon, J. Cho, D.H. Kang, Mater. Res. Bull. 34 (1999) 1451–1459.
[27] K. Ohshima, K. Tsuto, K. Okuyama, N. Tohge, Aerosol Sci. Technol. 19 (1993) 468–477.
[28] D.L. Liao, B.Q. Liao, J. Photochem. Photobiol. A: Chem. 187 (2007) 363–369.
[29] D.L. Liao, B.Q. Liao, Int. J. Chem. Reactor Eng. 5 (2007) 1–17 (Article 24).
[30] Y.J. Li, X.D. Li, J.W. Li, J. Yin, Water Res. 40 (2006) 1119–1126.
[31] J. Matos, J. Laine, J.M. Hermann, Appl. Catal. B: Environ. 18 (1998) 281–291.
[32] P.D. Cozzoli, A. Kornowski, H. Welleri, J. Am. Chem. Soc. 125 (2003) 14539–14548.
[33] J.N. Hay, H.M. Raval, Chem. Mater. 13 (2001) 3396–3403.
[34] G. Oskam, A. Nellore, R. Lee Penn, J. Phys. Chem. B 107 (2003) 1734–1738.
[35] T.J. Boyle, R.P. Tyner, T.M. Alam, J. Am. Chem. Soc. 121 (1999) 12104–12112.
[36] A. Hagfeldt, M. Gratzel, Chem. Rev. 95 (1995) 49–68.
[37] D. Morris, Y. Dou, J. Rebane, C.E.J. Mitchell, R.G. Egdell, D.S.L. Law, A. Vittadini, M. Casarin, Phys. Rev. B 61 (2000) 13445–13465.
[38] N. Serpone, P. Maruthamuthu, P. Pichat, E. Pelizzetti, H.J. Hidaka, J. Photochem. Photobiol. A: Chem. 85 (1995) 247–252.
[39] V. Sukharev, R. Kershaw, J. Photochem. Photobiol. A: Chem. 98 (1996) 165–169.
[40] J.G. Yu, H.G. Yu, B. Chen, X.J. Zhao, J.C. Yu, W.K. Ho, J. Phys. Chem. B 107 (2003) 13871–13879.
[41] J.G. Yu, J.C. Yu, W.K. Ho, Z.T. Jiang, New J. Chem. 26 (2002) 607–614.